The PedS2/PedR2 two-component system is crucial for the rare earth element switch in *Pseudomonas putida* KT2440

Matthias Wehrmann[a], Charlotte Berthelot[b,c], Patrick Billard[b,c], Janosch Klebensberger[a]#

[a]*University of Stuttgart, Institute of Technical Biochemistry, Stuttgart, Germany*

[b]*Université de Lorraine, LIEC UMR7360, Faculté des Sciences et Technologies, Vandoeuvre-lès-Nancy, France*

[c]*CNRS, LIEC UMR7360, Faculté des Sciences et Technologies, Vandoeuvre-lès-Nancy, France*

Running title: Rare earth element switch in *Pseudomonas putida*

#Address correspondence to Janosch Klebensberger, janosch.klebensberger@itb.uni-stuttgart.de.

Keywords: Lanthanides, rare earth element switch, signal transduction, *Pseudomonas putida*, PQQ, two-component regulatory system, PedS2, PedR2, histidine kinase, LuxR-type regulator, dehydrogenases, periplasm

ABSTRACT

In *Pseudomonas putida* KT2440, two pyrroloquinoline quinone-dependent ethanol dehydrogenases (PQQ-EDHs) are responsible for the periplasmic oxidation of a broad variety of volatile organic compounds (VOCs). Depending on the availability of rare earth elements (REEs) of the lanthanide series (Ln^{3+}), we have recently described that the transcription of the genes encoding the Ca^{2+}-utilizing enzyme PedE and the Ln^{3+}-utilizing enzyme PedH are inversely regulated. With adaptive evolution experiments, site-specific mutations, transcriptional reporter fusions, and complementation approaches, we herein demonstrate that the PedS2/PedR2 (PP_2671/PP_2672) two-component system (TCS) plays a central role in the observed REE-mediated switch of PQQ-EDHs in *P. putida*. We provide evidence that in the absence of lanthanum (La^{3+}), the sensor histidine kinase PedS2 phosphorylates its cognate LuxR-type response regulator PedR2, which in turn not only activates *pedE* gene transcription but is also involved in repression of *pedH*. Our data further suggests that the presence of La^{3+} lowers kinase activity of PedS2, either by the direct binding of the metal ions to the periplasmic region of PedS2 or by an uncharacterized indirect interaction, leading to reduced levels of phosphorylated PedR2. Consequently, the fading *pedE* expression and concomitant alleviation of *pedH* repression causes – in conjunction with the transcriptional activation of the *pedH* gene by a yet unknown regulatory module – the Ln^{3+}-dependent transition from PedE to PedH catalysed oxidation of alcoholic VOCs.

37 # IMPORTANCE

38 The function of lanthanides for methano- and methylotrophic bacteria is gaining increasing
39 attention, while knowledge about the role of rare earth elements (REEs) in non-
40 methylotrophic bacteria is still limited. The present study investigates the recently described
41 differential expression of the two PQQ-EDHs of *P. putida* in response to lanthanides. We
42 demonstrate that a specific TCS is crucial for their inverse regulation and provide evidence
43 for a dual regulatory function of the LuxR-type response regulator involved. Thus, our study
44 represents the first detailed characterization of the molecular mechanism underlying the
45 REE switch of PQQ-EDHs in a non-methylotrophic bacterium and stimulates subsequent
46 investigations for the identification of additional genes or phenotypic traits that might be co-
47 regulated during REE-dependent niche adaptation.

48 # INTRODUCTION

49 In its natural soil habitat, *Pseudomonas putida* KT2440 is exposed to a broad range of
50 potential carbon and energy sources (Regenhardt *et al.*, 2002; Wackett, 2003; Wu *et al.*,
51 2011), including plant-, fungi-, or bacterially derived volatile organic compounds (VOCs) with
52 alcohols or aldehydes as functional groups (Insam and Seewald, 2010; Penuelas *et al.*, 2014;
53 van Dam *et al.*, 2016). For efficient capture and metabolism of such VOCs, *P. putida* makes
54 use of two PQQ-dependent ethanol dehydrogenases (PQQ-EDHs) – namely PedE and PedH –
55 to carry out the initial oxidation steps in the periplasm of the cell (Mückschel *et al.*, 2012;
56 Wehrmann *et al.*, 2017). In a recent study, we found that these two type I quinoproteins
57 (Anthony, 2001; Toyama *et al.*, 2004) exhibit a similar substrate scope, but require different
58 metal cofactors for their catalytic activity (Wehrmann *et al.*, 2017). In contrast to PedE,
59 which uses Ca^{2+} ions, PedH was characterized as a rare earth element (REE)-dependent
60 enzyme that relies on the presence of lanthanide (Ln^{3+}) ions for catalytic activity. Notably,
61 due to their low solubility in most natural environments, REEs have long been considered to
62 have no biological function (Sarkar, 2002). However, the discovery of the wide-spread
63 occurrence of the REE-dependent XoxF-type of PQQ-dependent methanol dehydrogenases
64 (PQQ-MDHs), together with the more recent description of Ln^{3+}-dependent ethanol
65 dehydrogenases, has highlighted the important role of REEs for many bacterial species in
66 various environmental compartments (Fitriyanto *et al.,* 2011a; Fushimi, *et al.*, 2011; Pol *et*
67 *al.*, 2014; Taubert *et al.*, 2015; Chu and Lidstrom, 2016; Good *et al.*, 2016; Vekeman *et al.*,
68 2016; Shiller *et al.*, 2017; Wehrmann *et al.*, 2017; Lv *et al.*, 2018; Masuda *et al.*, 2018).
69 While in the absence of Ln^{3+} the oxidation of methanol in methylotrophs is driven by Ca^{2+}-
70 dependent PQQ-MDHs (MxaF-type), the presence of low amounts of REE ions is usually
71 sufficient to trigger a transcriptional switch to the XoxF-type of PQQ-MDHs. This inverse

72 regulation, called the REE switch, has been described for many methano- and/or
73 methylotrophic organisms (Farhan Ul Haque *et al.*, 2015; Chu and Lidstrom, 2016; Vu *et al.*,
74 2016; Gu and Semrau, 2017; Masuda *et al.*, 2018; Zheng *et al.*, 2018). From the growing
75 number of studies, it has become apparent that the molecular mechanism underlying this
76 switch for PQQ-MDHs is complex and can substantially differ among species. For example,
77 the inverse regulation in the non-methanotrophic methylotroph *Methylobacterium*
78 *extorquens* strain AM1 is controlled by two different two-component systems (TCS) (MxcQE
79 and MxbDM) and the orphan response regulator MxaB (Xu *et al.*, 1995; Springer *et al.*, 1997,
80 1998). In this organism it has been found that the transcriptional activation of both enzymes,
81 the Ca^{2+}-dependent MxaF and the two Ln^{3+}-dependent XoxF1 and XoxF2, is entirely lost in a
82 Δ*xoxF1*Δ*xoxF2* double mutant (Skovran *et al.*, 2011). As a consequence, a complex and
83 consecutive regulation was postulated, in which the different binding affinities of the *apo*
84 (no Ln^{3+} bound to the enzyme) and *holo* (Ln^{3+} bound to the enzyme) form of the XoxF
85 proteins to the periplasmic domain of the sensor histidine kinase MxcQ is essential to
86 regulate the switch (Vu *et al.*, 2016).
87 The type I methanotroph *Methylomicrobium buryatense* strain 5GB1C is lacking homologs of
88 the aforementioned TCS systems MxcQE and MxbDM (Chu and Lidstrom, 2016). In this
89 organism, the REE switch is regulated predominantly by the sensor histidine kinase MxaY
90 (Chu *et al.*, 2016). Chu and coworkers found that the activation of MxaY in the absence of
91 lanthanum activates the transcription of the Ca^{2+}-dependent enzyme MxaF by a so-far
92 unknown response regulator. In addition, the deletion of MxaY was found to almost entirely
93 eliminate the Ln^{3+}-mediated transcriptional activation of the Ln^{3+}-dependent enzyme XoxF in
94 a partially MxaB-dependent manner that also results in a severe growth defect, both in the
95 absence and presence of Ln^{3+}. As an additional layer of complexity, recent studies found that

96 the presence of other metal ions such as copper, which is needed as a cofactor for the
97 membrane-bound or particulate methane monooxygenase (pMMO) in methanotrophs, can
98 significantly impact the REE-mediated switch (Farhan Ul Haque *et al.*, 2015; Gu and Semrau,
99 2017; Semrau *et al.*, 2018).
100 In contrast to the increasing knowledge about the regulation of PQQ-MDHs in
101 methylotrophs, the molecular basis underlying such a regulatory switch for PQQ-EDHs in
102 non-methylotrophic organisms is not established. In the present study, we identify the TCS
103 encoded by PP_2671/PP_2672 (hereinafter referred to as PedS2/PedR2 according to the
104 genetic nomenclature from Arias *et al.*, 2008), consisting of the sensor histidine kinase PedS2
105 and its cognate LuxR-type transcriptional response regulator PedR2, as an essential
106 regulatory module for the REE-mediated switch of PQQ-EDHs in *P. putida* KT2440. We
107 provide evidence that the activity of PedS2 in the absence of lanthanides leads to
108 phosphorylation of PedR2 ($PedR2^P$), which serves a dual regulatory function. On the one
109 hand, $PedR2^P$ acts as a strong transcriptional activator of the *pedE* gene, which is essential to
110 allow growth with 2-phenylethanol in the absence of Ln^{3+}. At the same time, $PedR2^P$ also
111 functions as a repressor of *pedH*. From our data, we conclude that the presence of Ln^{3+} ions
112 triggers a reduction in PedS2 activity, either by a direct binding of the metal to the
113 periplasmic region of PedS2 or by an uncharacterized indirect interaction. This reduction of
114 PedS2 activity, together with a proposed phosphatase activity of PedS2 in its inactivated
115 state, causes the accumulation of non-phosphorylated PedR2, which over-time results in the
116 loss of the regulatory activity of the protein, and facilitates – in concert with the positive
117 feedback function of PedH in the presence of Ln^{3+} ions – the switch between PedE and PedH-
118 dependent growth.

119 # RESULTS

120 ***Identification of the sensor histidine kinase PedS2 as a lanthanide-responsive sensor***

121 As a consequence of the inverse regulation of *pedE* and *pedH*, a *pedH* deletion strain does
122 not grow within 48 h with 2-phenylethanol as sole carbon source in the presence of a critical
123 concentration of La^{3+} in the culture medium (Wehrmann *et al.*, 2017). To test whether
124 strains can be evolved, which are capable of overcoming the repression of *pedE* in the
125 presence of Ln^{3+} ions, an adaptive evolution experiment was performed (see **Figure 1** for a
126 general scheme).

127 When Δ*pedH* cultures were incubated with 2-phenylethanol in the presence of 10 µM La^{3+}
128 ions for longer than 5 d, growth was observed, indicating the occurrence of adapted strains
129 (data not shown). When independent clones were isolated from such cultures and passaged
130 several times on LB agar medium, their growth phenotype with 2-phenylethanol was still
131 much faster (< 2 d) than that observed for their Δ*pedH* parental strain and very similar to the
132 growth phenotype of the wild-type strain KT2440. Similar spontaneous suppressor mutants
133 have been described recently in methylotrophic organisms such as *M. extorquens* strain
134 AM1, *M. buryatense strain* 5GB1C, and *M. aquaticum* strain 22A during growth with
135 methanol (Chu and Lidstrom, 2016; Chu *et al.*, 2016; Masuda *et al.*, 2018). In *M. buryatense*,
136 whole genome sequencing revealed that the suppressor mutant strain was characterized by
137 a mutation in the membrane bound two-component sensor histidine kinase MxaY (Chu *et*
138 *al.*, 2016). In *P. putida* KT2440, the gene PP_2671 (hereinafter referred to as *pedS2*), located
139 in close genomic proximity to *pedE* (PP_2674), encodes a membrane bound histidine kinase
140 sharing 25 % amino acid sequence identity with MxaY (**Figure 1D-F**). To test the hypothesis
141 that mutations in *pedS2* are responsible for the emergence of suppressor phenotypes in
142 strain Δ*pedH* during growth in the presence of La^{3+}, the gene was sequenced in three

143 individually isolated mutants (Δ*pedH*$^{S1-3}$) (**Figure 1A-D**). This analysis revealed that all strains
144 contained a mutation in the *pedS2* sequence leading to a non-synonymous substitution.
145 These mutations were either located within a predicted periplasmic domain of unknown
146 function (R73C [Δ*pedH*^{S1}] and R111W [Δ*pedH*^{S2}]) or within the HAMP domain (S178P
147 [Δ*pedH*^{S3}]), which is responsible for signal transduction from the periplasm into the
148 cytoplasm of the cell (Stock *et al.*, 2000; Parkinson, 2010). To verify that the identified
149 mutations in *pedS2* are the primary cause of the suppressor phenotype, the S178P mutation
150 from Δ*pedH*^{S3} was introduced into the genetic background of strain Δ*pedH*, resulting in strain
151 Δ*pedH*_PedS^{S178P}.
152 In subsequent growth experiments with 2-phenylethanol in the absence of La^{3+}, strains
153 Δ*pedH* and Δ*pedH*_PedS2^{S178P} showed a similar growth behavior with a lag phase of < 32 h
154 (**Figure 2A1**; **Figure 2A2**). In the presence of 10 µM La^{3+}, however, Δ*pedH* showed no growth
155 within 72 h, whereas Δ*pedH*_PedS2^{S178P} reached its maximum optical densities again after
156 about 32 h of incubation, verifying that the observed mutation in the histidine kinase *pedS2*
157 was sufficient to cause the suppressor phenotype. We speculated that the LuxR-type
158 response regulator PP_2672 (hereinafter referred to as *pedR2*), which is located adjacent to
159 *pedS2* within the genome of *P. putida* KT2440, represents the target of PedS2 activity. This
160 assumption is based on the fact that PedR2 represents a homologue (65% amino acid
161 sequence identity) of EraR (ExaE; PA1980), which forms a TCS with the cytosolic histidine
162 kinase EraS (ExaD; PA1979) that activates expression of the *pedE* homologue *exaA* in
163 *Pseudomonas aeruginosa* (Schobert and Görisch, 2001; Mern *et al.*, 2010). To test this
164 hypothesis, *pedS2* as well as its potential cognate response regulator encoding gene *pedR2*,
165 were deleted in a Δ*pedH* background. In addition, strains suitable for probing promoter
166 activity of *pedE* in strains Δ*pedH,* Δ*pedH*_PedS2^{S178P}, Δ*pedH*Δ*pedS2* and Δ*pedH*Δ*pedR2* were

167 constructed and subsequently analyzed during growth with 2-phenylethanol in the presence
168 and absence of La^{3+} (**Figure 2B**).

169 ***The TCS PedS2/PedR2 regulates pedE transcription in response to lanthanide availability***

170 In accordance with the observed growth patterns, *pedE* promoter activities in strain
171 Δ*pedH*_PedS2^{S178P} were almost identical in both the absence and the presence of La^{3+} (ratio
172 no La^{3+} to 1 µM La^{3+}: 0.89 ± 0.02) but increased more than 24-fold (24 ± 1 and 27 ± 1-fold,
173 respectively) compared to the *pedE* promoter activities determined for cells of strain Δ*pedH*
174 in the absence of La^{3+} (**Figure 2B**). Strain Δ*pedH*Δ*pedS2* also showed a La^{3+}-independent
175 growth phenotype similar to strain Δ*pedH*_PedS2^{S178P}, however with a clear delay (< 48 h vs.
176 < 32 h) (**Figure 2A3**). Promoter activities for *pedE* were almost identical in this strain in the
177 absence and presence of La^{3+} (ratio no La^{3+} to 1 µM La^{3+}: 1.07 ± 0.09) (**Figure 2B**).
178 In contrast, incubations of 72 h (**Figure 2A4**) or even prolonged incubations for more than 7
179 d (data not shown) did not result in detectable growth of strain Δ*pedH*Δ*pedR2* with 2-
180 phenylethanol, both in the presence and absence of La^{3+}. Correspondingly, *pedE* promoter
181 activities in this strain were low compared to those observed for cells of strain Δ*pedH* in the
182 presence of La^{3+} but in a similar range as those observed for Δ*pedH*Δ*pedS2* in the presence
183 and absence of La^{3+}. These data demonstrate that the PedS2/PedR2 system is the
184 predominant element in the La^{3+}-dependent regulation of *pedE* and that PedR2 is essential
185 for PedE-dependent growth. However, as PedE-dependent growth can still be observed in
186 the absence of PedS2 after prolonged incubations and in a PedR2-dependent manner (**Figure
187 2A3; Figure 2A4**), we assume that at least one additional lanthanide-independent kinase
188 must be able to phosphorylate PedR2, leading to transcriptional activation of *pedE* and
189 functional production of the calcium-dependent enzyme under these conditions.

190 ***The TCS PedS2/PedR2 regulates the partial repression of pedH in the absence of***
191 ***lanthanides***

192 Based on the critical role of PedS2/PedR2 in the regulation of *pedE* and the fact that LuxR-
193 type regulators have been demonstrated to be capable of acting as both transcriptional
194 activators and repressors (Waters and Bassler, 2006; Van Kessel *et al.*, 2013), we speculated
195 that this TCS could also be involved in the regulation of *pedH*. To test this hypothesis, strains
196 Δ*pedE*_PedS2^{S178P}, Δ*pedE*Δ*pedS2*, and Δ*pedE*Δ*pedR2* were generated and a transcriptional
197 reporter suitable for probing *pedH* promoter activities was integrated into the genome of
198 each of these strains.

199 Experiments with 2-phenylethanol revealed that strains Δ*pedE*, Δ*pedE*Δ*pedS2*, and
200 Δ*pedE*Δ*pedR2* showed La^{3+}-dependent growth after a lag-phase < 24 h and reached the
201 maximum OD_{600} after ≤ 32 h (**Figure 3A1**; **Figure 3A3**; **Figure 3A4**). In contrast, strain
202 Δ*pedE*_PedS2^{S178P} exhibited an extended lag-phase (> 24 h) and consistently reached the
203 maximal OD_{600} only after prolonged incubations (≥ 32 h; **Figure 3A2**). In accordance with
204 these growth results, *pedH* promoter activities of strains Δ*pedE*, Δ*pedE*Δ*pedS2,* and
205 Δ*pedE*Δ*pedR2* were in a similar range, whereas *pedH* promoter activities in strain
206 Δ*pedE*_PedS2^{S178P} were 45 ± 2-fold and 30 ± 2-fold lower than strain Δ*pedE* in absence or
207 presence of La^{3+}, respectively (**Figure 3B**). Assuming that the S178P mutation in PedS2
208 results in a sensor kinase activity that mimics that of the wild-type protein in the absence of
209 lanthanides, it is very likely that PedS2 is responsible for the repression of *pedH* under the
210 La^{3+}-free conditions leading to the observed delay in growth. To find out whether this
211 regulatory effect on *pedH* proceeds *via* the response regulator PedR2, as it is the case for
212 *pedE*, or is caused by an unknown additional target of PedS2, the triple mutant strain
213 Δ*pedE*_PedS2^{S178P}Δ*pedR2* was generated and characterized for its growth phenotype (**Figure**

214 **4A**). In this experiment, Δ*pedE* and Δ*pedE*_PedS2^{S178P} both grew with 2-phenylethanol,
215 however, with a clear difference in the corresponding lag-phases confirming the previous
216 results from growth in 96-well plates (**Figure 3A**). In contrast, the additional deletion of the
217 response regulator PedR2 eliminated the growth defect caused by the PedS2^{S178P} allele,
218 leading to a growth behavior of Δ*pedE*_PedS2^{S178P}Δ*pedR2* (**Figure 4A**), which was
219 indistinguishable from that of strain Δ*pedE*.

220 **The conserved phosphorylation site D53 in PedR2 is essential for the REE-mediated switch**

221 In order to study the essentiality of the phosphorylation site at position D53 of PedR2
222 (Bourret *et al.*, 1990; Milani *et al.*, 2005), we used inducible constructs for the production of
223 the wild-type PedR2 protein (pJEM[PedR2]) and a mutated variant, in which the conserved
224 aspartate in the CheY-like receiver domain was replaced by an alanine (pJEM[PedR2^{D53A}]).
225 After transformation of these plasmids into strains Δ*pedH*Δ*pedR2* and
226 Δ*pedE*_PedS2^{S178P}Δ*pedR2* their growth with 2-phenylethanol in the absence and presence of
227 La^{3+} was monitored. When the plasmid-borne wild-type regulator PedR2 was induced in cells
228 of Δ*pedH*_PedS2^{S178P}Δ*pedR2,* growth was observed after a lag-phase of < 24 h whereas the
229 PedR2^{D53A} variant was unable to restore PedE-dependent growth in the same strain (**Figure**
230 **4B**). Intriguingly, the reverse result was obtained in strain Δ*pedE*_PedS2^{S178P}Δ*pedR2*. Here,
231 the PedR2^{D53A} variant allowed PedH-dependent growth, whereas the wild-type regulator
232 PedR2 did not lead to significant growth within 120 h of incubation (**Figure 4C**).

233 # DISCUSSION

234 We recently demonstrated that in *P. putida* KT2440 the production of the two PQQ-EDHs
235 PedE and PedH is both tightly and inversely regulated depending on lanthanide availability,
236 representing the first reported REE switch for PQQ-EDHs in a non-methylotrophic organism
237 (Wehrmann *et al.*, 2017). While we were able to show that Ln^{3+}-dependent transcriptional
238 activation of *pedH* is mostly, but not entirely, dependent on the presence of the PedH
239 protein itself, the Ln^{3+}-dependent transcriptional repression of *pedE* remained elusive. In this
240 study, we present a detailed characterization of the mechanism underlying PedE and PedH
241 regulation (**Figure 5**), in which the TCS PedS2/PedR2 acts as an essential signaling module for
242 the REE-mediated switch between the two quinoproteins. Similar to the recently
243 characterized spontaneous mutant of *M. buryatense* (Chu *et al.*, 2016), we found that a
244 single non-synonymous mutation within the periplasmic region of the sensor histidine kinase
245 PedS2 ($PedS2^{S178P}$), which differs from the LapD/MoxY domain found in MxaY of *M.*
246 *buryatense* (**Figure 1**), is sufficient to terminate the Ln^{3+}-mediated repression of *pedE*.
247 Notably, various mutations at different sites of the protein can cause the observed
248 suppressor phenotype. This might explain the repeatedly and fast occurrence of these
249 suppressor mutants in our experiments and would support a similar notion in *M. buryatense*
250 (Chu and Lidstrom, 2016; Chu *et al.*, 2016).

251 Besides the essentiality for *pedE* regulation, our experimental data further provide strong
252 evidence that PedS2 is also involved in the repression of *pedH* in the absence of lanthanides,
253 but not in its Ln^{3+}-dependent activation. This is based on the observation that the
254 Δ*pedE*Δ*pedS2* deletion strain did not show any differences in growth and *pedH* regulation,
255 while the suppressor mutant Δ*pedE*_$PedS2^{S178P}$ displayed decreased *pedH* promoter activity
256 and a strongly increased lag-phase in growth experiments in the presence of La^{3+}. We

257 additionally show that the *pedS2*-dependent regulations of *pedE* and *pedH* are both
258 mediated by the LuxR-type response regulator PedR2. From these data we conclude that in
259 absence of La^{3+} ions the PedS2 sensor histidine kinase is active and triggers phosphorylation
260 of PedR2 at the conserved position D53 ($PedR2^{P}$) (Bourret *et al.*, 1990; Milani *et al.*, 2005).
261 The phosphorylated state of PedS2 subsequently has a dual regulatory function, namely the
262 activation of *pedE* and concomitant repression of *pedH* transcription (**Figure 5A**). In this
263 context, it is interesting to note that expression of the gene *exaA* in *Azospirillum brasilense*
264 Sp7, which encodes for a PQQ-dependent alcohol dehydrogenase, is dependent on σ^{54} and
265 its interaction with a LuxR-type response regulator that shares 45% sequence identity with
266 PedR2 (Singh *et al.*, 2017). Whether the transcriptional activation of *pedE* is dependent on a
267 similar interaction of PedR2 with a specific sigma factor is currently unknown.
268 To our surprise, also a Δ*pedH*Δ*pedS2* mutant was able to grow on 2-phenylethanol, even
269 though with an increased lag-phase and low *pedE* promoter activities (**Figure 2A3**). This
270 indicates that at least one additional kinase beside PedS2 must be capable of
271 phosphorylating PedR2 to facilitate growth of this strain under these conditions. Given that
272 such an additional kinase exists, it is surprising that a *pedH* single mutant, in contrast to the
273 aforementioned Δ*pedH*Δ*pedS2* double mutant, is only able to grow in the presence of REEs
274 when PedS2 is mutated (e.g. $PedS2^{S178P}$; **Figure 2A1)**. This suggests that the activity of the
275 additional, non-specific histidine kinase towards PedR2 in the presence of La^{3+} is repressed
276 as long as PedS2 is functional. We hence propose that PedS2, as many other sensory
277 histidine kinases in bacteria (Stock *et al.*, 2000; Rowland and Deeds, 2014; Agrawal *et al.*,
278 2016), also exhibits phosphatase activity on $PedR2^{P}$ in the presence of La^{3+}, thereby ensuring
279 specificity of the signal transduction pathway and eliminating the interference from other
280 non-specific kinases. In our working hypothesis, the presence of lanthanides in the medium

281 leads to the repression of PedS2 kinase activity, most likely by direct binding of the metal
282 ions to its periplasmic domain (**Figure 5B**). The reduced kinase- and postulated phosphatase
283 activity of PedS2 consequently leads to the accumulation of unphosphorylated PedR2, which
284 finally results in the loss of its regulatory functions. In addition, the transcription of *pedH* is
285 activated *via* a yet unknown pathway, in which a functional PedH protein is an essential
286 component most likely by acting as a lanthanide sensor (Wehrmann *et al.*, 2017).
287 In conclusion, it appears that the REE-mediated switches in *M. extorquens* AM1 and *M.*
288 *buryatense* during growth with methanol are predominantly dependent on only one
289 lanthanide responsive pathway, which either proceeds via the XoxF1 and XoxF2 proteins or
290 MxaY (Chu *et al.*, 2016; Vu *et al.*, 2016). Our results establish that in *P. putida* KT2440, a
291 combination of at least two independent pathways are important to orchestrate the inverse
292 regulation of *pedE* and *pedH* in response to lanthanides efficiently.
293 Several recent studies suggest that in methano- and methylotrophic bacteria, the REE switch
294 might affect more genes than only those needed for the periplasmic oxidation system itself
295 (Gu and Semrau, 2017; Good *et al.*, 2018; Masuda *et al.*, 2018). Reports on physiological
296 consequences are, however, inconsistent as some studies found no effects (Nakagawa *et al.*,
297 2012; Chu and Lidstrom, 2016; Vu *et al.*, 2016; Masuda *et al.*, 2018), whereas other studies
298 reported a stimulating effect on biofilm formation, growth rates, and overall yields in the
299 presence of REE (Fitriyanto *et al.*, 2011b; Nakamura, *et al.*, 2011; Good *et al.*, 2018). We
300 think it is not unlikely that additional REE-mediated regulatory effects do also exist in *P.*
301 *putida* KT2440 in a context-dependent manner. Thus, one of our current foci is to investigate
302 the global regulatory impact and physiological consequences of the presence and absence of
303 lanthanides under varying environmental conditions.

304 # MATERIAL AND METHODS

305 ***Bacterial strains, plasmids and culture conditions***

306 A detailed description of the strains and plasmids used in this study can be found in **Table 1**.
307 If not stated otherwise *Escherichia coli* and *P. putida* KT2440 strains were maintained on
308 solidified LB medium. Routinely, strains were cultured in liquid LB medium (Maniatis *et al.*,
309 1982) or a modified M9 salt medium (Wehrmann *et al.*, 2017) supplemented with 25 mM
310 succinate or 5 mM 2-phenylethanol as source of carbon and energy at 30°C and shaking, if
311 not stated otherwise. For maintenance and selection, 40 µg mL^{-1} kanamycin or 15 µg mL^{-1}
312 gentamycin for *E.coli* and 40 µg mL^{-1} kanamycin, 20 µg mL^{-1} 5-fluoro uracil, or 15 µg mL^{-1}
313 gentamycin for *P. putida* strains was added to the medium, if indicated.

314 ***Liquid medium growth experiments***

315 All liquid growth experiments were carried out using modified M9 with 25 mM succinate or
316 5 mM 2-phenylethanol as sole source of carbon and energy (see above) in 125 ml or 250 ml
317 polycarbonate Erlenmeyer flask (Corning) or in 96-well 2 ml deep-well plates (Carl Roth), as
318 described previously (Wehrmann *et al.*, 2017). Briefly, washed cells from overnight cultures
319 grown with succinate at 30°C and 180 rpm shaking were used to inoculate fresh medium
320 with an OD_{600} of 0.01 and incubated at 30°C and 180 rpm (growth experiments in
321 polycarbonate Erlenmeyer flasks) or 350 rpm (growth experiments in 96-well plates)
322 shaking.

323 ***Construction of plasmids***

324 For construction of the deletion plasmids pMW55, pMW56 and pMW61 the 600 bp regions
325 upstream and downstream of gene *pedS2* (*PP_2671*), amino acid residue S178 in gene *pedS2*
326 (*PP_2671*), or gene *pedR2* (*PP_2672*) were amplified from genomic DNA of *P. putida* KT2440

327 using primers MWH90-93, MWH98-101 or MWH106-109 (**Table 1**). The two up- and
328 downstream fragments and BamHI digested pJOE6261.2 were then joined together using
329 one-step isothermal assembly (Gibson, 2011). Upon subsequent transformation of the
330 constructs into *E. coli* BL21(DE3) cells, the correctness of the plasmids was confirmed by
331 Sanger sequencing. Plasmids pJeM[pedR2] and pJEM[PedR2^{D53A}] encoding for PedR2 or
332 PedR2 with mutated amino acid residue 53 (D→A) under a rhamnose inducible promoter
333 were ordered from an external source (Eurofins).

334 ***Strain constructions and isolation of suppressor mutants***

335 The *pedS2* (*PP_2671*) and *pedR2* (*PP_2672*) negative mutants as well as the PedS2^{S178P} allele
336 were constructed using a recently described system for markerless gene deletion in *P. putida*
337 KT2440 (Graf and Altenbuchner, 2011). Briefly, the integration vectors harboring the up- and
338 downstream regions of the target genes (pMW55 and pMW61) or the up- and downstream
339 regions of the region to be mutated including the desired S178P mutation (pMW56) were
340 transformed into *P. putida* KT2440* and kanamycin (Kan) resistant and 5-flourouracil (5-FU)
341 sensitive clones were selected on LB Kan agarose plates. After incubation at 30°C for 24 h in
342 LB medium without selection markers, clones that were 5-FU^{R} and Kan^{S} were tested for
343 successful gene deletion using primer pair MWH90/MWH93 or MWH106/MWH109 for gene
344 *pedS2* or *pedR2*, respectively. The presence of the underlying PedS2^{S178P} mutation was
345 verified by Sanger sequencing after gene *pedS2* of 5-FU^{R} and Kan^{S} clones was amplified using
346 primer pair MWH85/MWH86. Δ*pedH* suppressor mutant strains were isolated from 25 ml
347 liquid M9 cultures with 5 mM 2-phenylethanol as sole source of carbon and energy
348 supplemented with 10 µM La^{3+} upon > 5 d incubation at 30°C and 180 rpm. Strains were
349 passed thrice over LB agar plates and reevaluated for growth in liquid M9 medium
350 supplemented with 5 mM 2-phenylethanol and 10 µM La^{3+}. From cultures that showed

351 growth upon a similar lag-phase as the KT2440* wild-type strain, the *pedS2* gene was
352 amplified by PCR using primer pair M85/M86 and mutations were identified by Sanger
353 sequencing.
354 To construct reporter strains for the analysis of *pedE* and *pedH* promoter activity in different
355 genetic backgrounds, plasmids pUC18-mini-Tn*7*T-*pedE-lux-Gm* and pUC18-mini-Tn*7*T-*pedH-*
356 *lux-Gm* (Wehrmann *et al.*, 2017) were co-electroporated with the helper plasmid pTNS2 into
357 selected mutant strains of *P. putida* KT2440 (**Table 1**). Proper chromosomal integration of
358 the mini-Tn7 element in gentamycin resistant transformants was verified by colony PCR
359 using $P_{put\text{-}glmSDN}$ and P_{Tn7R} primers as described previously (Choi *et al.*, 2005).

360 ***Reporter gene fusion assays***

361 For quantitative measurement of *pedE* and *pedH* promoter activity, strains of *P. putida*
362 harboring a Tn*7*-based *pedE-lux* or *pedH-lux* transcriptional reporter fusion were grown
363 overnight in LB medium with gentamycin (15 $\mu g.ml^{-1}$), diluted to an OD_{600} = 0.2 in fresh LB
364 medium and grown to an OD_{600} of 0.6. Cells were then washed three times in M9 medium
365 without carbon source and finally adjusted to an OD_{600} of 0.2 in M9 medium with 1 mM 2-
366 phenylethanol. For luminescence measurements, 198 µl of cell suspension was added to 2 µl
367 of a 100 µM $LaCl_3$ solution in white 96-well plates with a clear bottom (µClear; Greiner Bio-
368 One). Microtiter plates were placed in a humid box to prevent evaporation and incubated at
369 28°C with continuous agitation (180 rpm), and light emission and OD_{600} were recorded at
370 regular intervals in an FLX-Xenius plate reader (SAFAS, Monaco) for 6 h. For both
371 parameters, the background provided by the M9 medium was subtracted and the
372 luminescence was normalized to the corresponding OD_{600}. Experiments were performed
373 with biological triplicates, and data are presented as the mean value with error bars
374 representing the corresponding standard deviation.

375 ***Sequence identity determination***

376 Protein sequence identities were determined based on amino acid sequence alignments of
377 the proteins of interest generated using the Clustal Omega multiple sequence alignment tool
378 (Sievers *et al.*, 2014).

379 FUNDING INFORMATION

380 The work of Matthias Wehrmann and Janosch Klebensberger was supported by an individual
381 research grant from the Deutsche Forschungsgemeinschaft (DFG, KL 2340/2-1). The work of
382 Charlotte Berthelot and Patrick Billard was supported in part by Labex Ressources21 (ANR-
383 10-LABX-21-01).

384 ACKNOWLEDGEMENTS

385 The authors would like to thank Prof. Bernhard Hauer for his continuous support. The
386 authors further declare that the research was conducted in the absence of any commercial
387 or financial relationships that could be construed as a potential conflict of interest.

388 # Tables

389 **Table 1:** Strain, plasmids, and primer used in the study

Strains	**Relevant features**
KT2440	Wild-type strain of *Pseudomonas putida* (ATCC 47054)
KT2440*	KT2440 with a markerless deletion of *upp* | Parent strain for deletion mutants (Graf and Altenbuchner, 2011)
Δ*pedE*	KT2440* with a markerless deletion of *pedE* (Mückschel *et al.*, 2012)
Δ*pedE*Δ*pedS2*	Δ*pedE* with a markerless deletion of *pedS2* (*PP_2671*) (this study)
Δ*pedE*Δ*pedR2*	Δ*pedE* with a markerless deletion of *pedR2* (*PP_2672*) (this study)
Δ*pedE*_PedS2^{S178P}	Δ*pedE* with S178P mutation in PedS2 (this study)
Δ*pedE*_PedS2^{S178P}Δ*pedR2*	Δ*pedE*_PedS2^{S178P} with a markerless deletion of *pedR2* (this study)
Δ*pedH*	KT2440* with a markerless deletion of *pedH* (Mückschel *et al.*, 2012)
Δ*pedH*Δ*pedS2*	Δ*pedH* with a markerless deletion of *pedS2* (this study)
Δ*pedH*Δ*pedR2*	Δ*pedH* with a markerless deletion of *pedR2* (this study)
Δ*pedH*_PedS2^{S178P}	Δ*pedH* with S178P mutation PedS2 (this study)
Δ*pedH*_PedS2^{S178P}Δ*pedR2*	Δ*pedH*_PedS2^{S178P} with a markerless deletion of *pedR2* (this study)
E. coli BL21 (DE3)	*F⁻ ompT gal dcm lon hsdS$_B$(r$_B^-$ m$_B^-$) λ(DE3 [lacI lacUV5-T7 gene 1 ind1 sam7 nin5])*
E. coli DH5α	*fhuA2 lac(del)U169 phoA glnV44 Φ80' lacZ(del)M15 gyrA96 recA1 relA1 endA1 thi-1 hsdR17*
KT2440*::Tn7-*pedE-lux*	KT2440* with insertion of miniTn7-*pedE-lux* (Wehrmann *et al.*, 2017)
KT2440*::Tn7-pedH-lux	KT2440* with insertion of miniTn7-*pedH*-lux (Wehrmann et al., 2017)
Δ*pedE*::Tn7-*pedE-lux*	Δ*pedE* with insertion of miniTn7-*pedE-lux* (Wehrmann *et al.*, 2017)
Δ*pedE*::Tn7-*pedH-lux*	Δ*pedE* with insertion of miniTn7-*pedH-lux* (Wehrmann *et al.*, 2017)
Δ*pedH*::Tn7-*pedE-lux*	Δ*pedH* with insertion of miniTn7-*pedE-lux* (Wehrmann *et al.*, 2017)
Δ*pedH* ::Tn7-*pedH-lux*	Δ*pedH* with insertion of miniTn7-*pedH-lux* (Wehrmann *et al.*, 2017)
Δ*pedE*Δ*pedS2*::Tn7-*pedH-lux*	Δ*pedE*Δ*pedS2* with insertion of miniTn7-*pedH-lux* (this study)
Δ*pedE*Δ*pedR2*::Tn7-*pedH-lux*	Δ*pedE*Δ*pedR2* with insertion of miniTn7-*pedH-lux* (this study)
Δ*pedE*_PedS2^{S178P} ::Tn7-*pedH-lux*	Δ*pedE*_PedS2^{S178P} with insertion of miniTn7-*pedH-lux* (this study)
Δ*pedH*Δ*pedS2*::Tn7-*pedE-lux*	Δ*pedH*Δ*pedS2* with insertion of miniTn7-*pedE-lux* (this study)
Δ*pedH*Δ*pedR2*::Tn7-*pedE-lux*	Δ*pedH*Δ*pedR2* with insertion of miniTn7-*pedE-lux* (this study)
Δ*pedH*_PedS2^{S178P} ::Tn7-*pedE-lux*	Δ*pedH*_PedS2^{S178P} with insertion of miniTn7-*pedE-lux* (this study)
Plasmids	
pJeM1	Rhamnose inducible vector (Jeske and Altenbuchner, 2010)
pJOE6261.2	Suicide vector for gene deletions (Graf and Altenbuchner, 2011)
pMW55	pJOE6261.2 based deletion vector for gene *PP_2671* (this study)
pMW56	pJOE6261.2 based vector for introducing the S178P mutation in PedS2 (this study)
pMW61	pJOE6261.2 based deletion vector for gene *PP_2672* (this study)
pUC18-mini-Tn*7*T-*pedE-lux-Gm*	pUC18-mini-Tn*7*T-Gm-lux vector with the promoter of *pedE* driving transcription of *luxCDABE* (Wehrmann *et al.*, 2017)

pUC18-mini-Tn*7*T-*pedH*-*lux*-Gm	pUC18-mini-Tn*7*T-*lux*-Gm vector with the promoter of *pedH* driving transcription of *luxCDABE* (Wehrmann *et al.*, 2017)	
pTNS2	Helper plasmid for Tn7 integration (Choi *et al.*, 2005)	
pJEM[PedR2]	Rhamnose inducible induction of PedR2 (this study)	
pJEM[PedR2^{D53A}]	Rhamnose inducible induction of PedR2^{D53A} (this study)	
Primer		
Name	**Sequence 5' → 3'**	**Annealing**
MWH85	GGAAATATGCAGAAAGTAGCGCTCG	60°C
MWH86	TCTTCACCACTGGCGGCCT	60°C
MWH90	GCCGCTTTGGTCCCGCAGGCACTGGCTGCTGC	60°C
MWH91	CGATATTCAAAGCGGTTCTCCTCAGGC	60°C
MWH92	GAACCGCTTTGAATATCGTGTTGGTCGATGACCAC	60°C
MWH93	GCAGGTCGACTCTAGAGGATGCACAAGCTCGGCG	60°C
MWH98	GCCGCTTTGGTCCCGAGGTAGTAATTCAGTGCGGGGG	60°C
MWH99	TGCCCGCCTGGGACCTGGTG	60°C
MWH100	GGTCCCAGGCGGGCAATTG	60°C
MWH101	GCAGGTCGACTCTAGAGGCAGCCATTGTCGCGAATG	60°C
MWH106	GCCGCTTTGGTCCCGGCAGGAGCAGGAGCGTAC	65°C
MWH107	TGAAATACCCACACCTCCTGGGGAATGTTAAG	65°C
MWH108	GGAGGTGTGGGTATTTCATTGCACCTGTTGGGGC	65°C
MWH109	GCAGGTCGACTCTAGAGGAGCCAACCTGACCC	65°C

390

391 # Figures

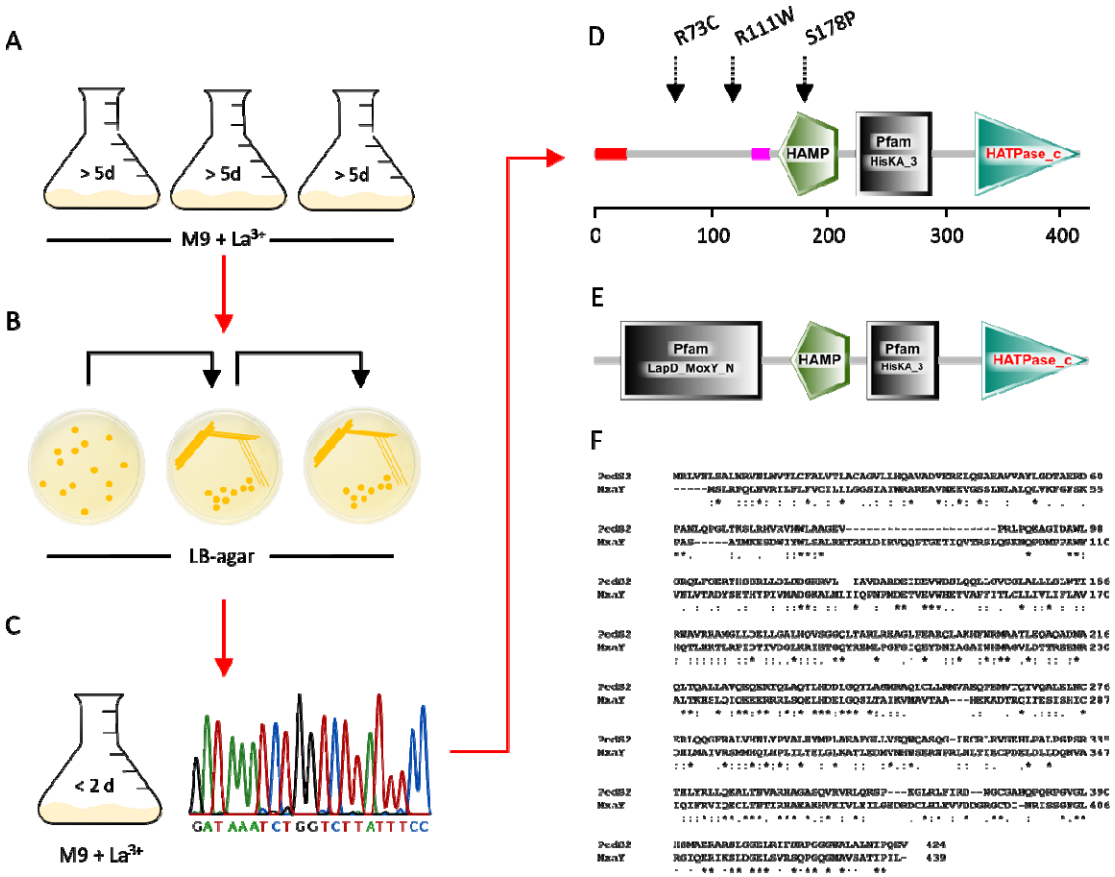

392

393 **Figure 1:** Scheme of selection (**A**), clonal isolation (**B**), characterization and single nucleotide

394 polymorphism (SNP) identification (**C-D**) in the two-component sensor histidine kinase PedS2

395 of the spontaneous mutants Δ*pedH*^{S1} (R73C), Δ*pedH*^{S2} (R111W), Δ*pedH*^{S3} (S178P). **A**) Cells of

396 strain Δ*pedH* were incubated in M9 medium supplemented with 5 mM 2-phenylethanol and

397 10 µM $LaCl_3$ in plastic Erlenmeyer flasks (n = 3) at 30°C with shaking at 180 rpm. **B**) After

398 growth was observed (> 5 days), dilutions from each culture were plated onto LB-agar plates

399 and incubated at 30°C. Individual clones were further streaked on LB-agar twice prior to

400 further characterization. **C**) Clones were characterized for their growth behavior in M9

401 medium with 5 mM 2-phenylethanol in the presence of 10 µM $LaCl_3$. Subsequently, one

402 clone from each culture exhibiting faster growth than the parental strain Δ*pedH* was used for

403 PCR amplification of the *pedS2* gene and multi sequence alignment analysis with the native
404 sequence of the gene from the *Pseudomonas* Genome Database (Winsor *et al.*, 2016). **D-E**)
405 Visualization of domain composition of PedS2 of *P. putida* (**D**) and MxaY of *M. buryatense*
406 5GB1C (**E**) using the prediction from the Simple Modular Architecture Research Tool (Letunic
407 and Bork, 2018). **F**) Amino acid sequence alignment of the PedS2 and MxaY proteins
408 generated with Clustal Omega (Sievers *et al.*, 2014).

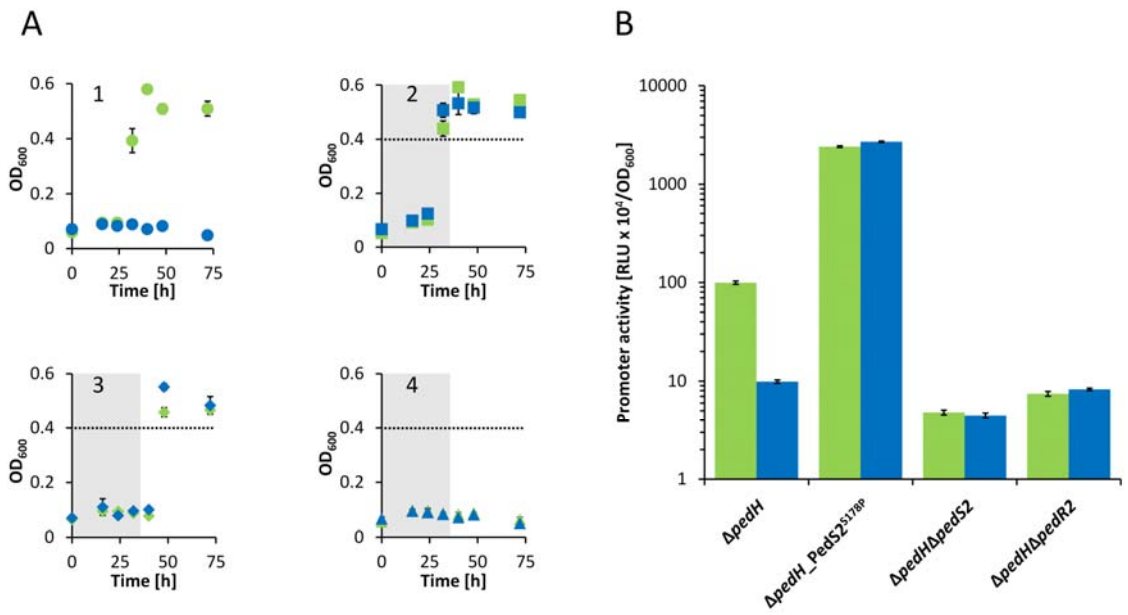

409

410 **Figure 2:** (**A**) Growth of strains Δ*pedH* (circles; 1), Δ*pedH_pedS2*^{S178P} (squares; 2),

411 Δ*pedH*Δ*pedS2* (diamonds; 3), and Δ*pedH*Δ*pedR2* (triangles; 4) at 30°C and 350 rpm shaking

412 with M9 medium in 96-well plates supplemented with 5 mM 2-phenylethanol in absence

413 (green symbols) or presence (blue symbols) of 10 µM La^{3+}. The grey area visualizes the time

414 point by which the parental strain Δ*pedH* (circles) reached an OD_{600} > 0.4 (dotted line) (**B**)

415 Activities of the *pedE* promoter in strains Δ*pedH,* Δ*pedH*_PedS2^{S178P}*,* Δ*pedH*Δ*pedS2,* and

416 Δ*pedH*Δ*pedR2* in the absence (green bars) or presence (blue bars) of 1 µM La^{3+} measured in

417 M9 medium supplemented with 1 mM 2-phenylethanol. Promoter activities are presented in

418 relative light units (RLU x 10^4) normalized to OD_{600}. All data represent the mean of biological

419 triplicates and error bars correspond to the respective standard deviations.

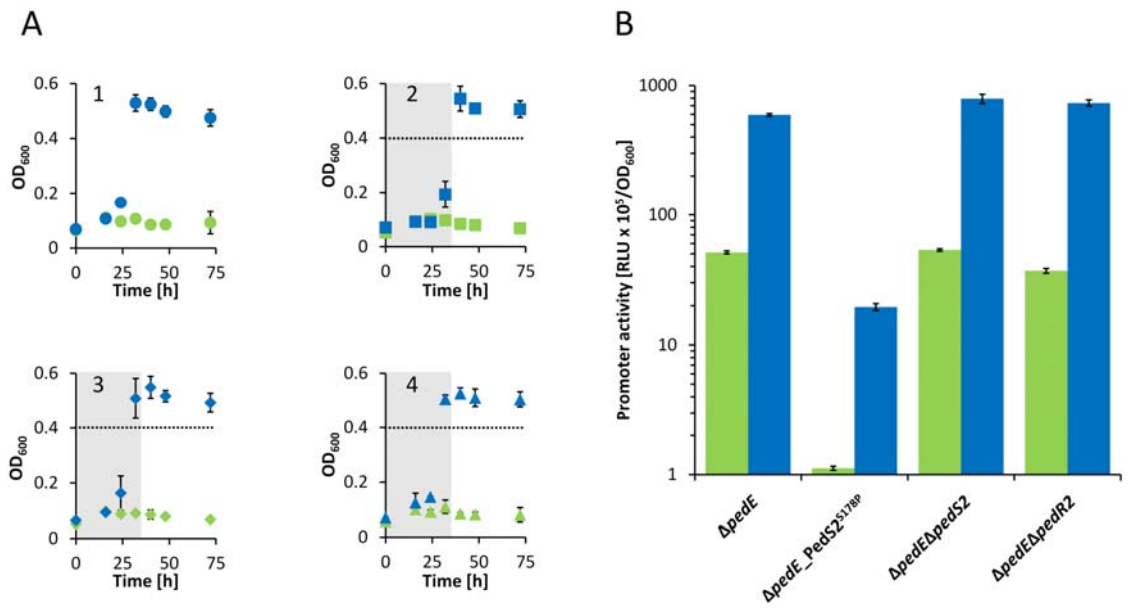

420

421 **Figure 3:** (**A**) Growth of strains Δ*pedE* (circles; 1), Δ*pedE*_PedS2^{S178P} (squares; 2),

422 Δ*pedE*Δ*pedS2* (diamonds; 3), and Δ*pedE*Δ*pedR2* (triangles; 4) at 30°C and 350 rpm shaking

423 with M9 medium in 96-well plates supplemented with 5 mM 2-phenylethanol in absence

424 (green symbols) or presence (blue symbols) of 10 µM La^{3+}. The grey area visualizes the time

425 point by which the parental strain Δ*pedE* (circles) reached their maximum OD_{600} (**B**) Activities

426 of the *pedH* promoter in strains Δ*pedE,* Δ*pedE*_PedS2^{S178P}*,* Δ*pedE*Δ*pedS2,* and Δ*pedE*Δ*pedR2*

427 in the absence (green bars) or presence (blue bars) of 1 µM La^{3+} measured in M9 medium

428 supplemented with 1 mM 2-phenylethanol. Promoter activities are presented in relative

429 light units (RLU x 10^5) normalized to OD_{600}. All data represent the mean of biological

430 triplicates and error bars correspond to the respective standard deviations.

431

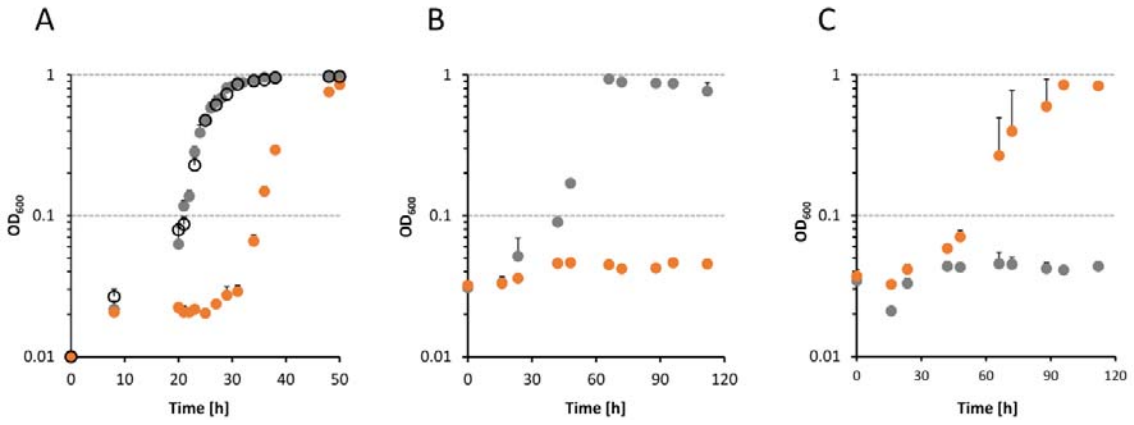

432

433 **Figure 4**: Growth of different *P. putida* strains at 30°C and 180 rpm shaking with M9 medium

434 in polycarbonate Erlenmeyer flasks supplemented with 5 mM 2-phenylethanol and 10 µM

435 La^{3+} in the absence (**A**) and presence of kanamycin (**B** and **C**) for plasmid maintenance. Flasks

436 were inoculated at an OD_{600} of 0.01 (**A**) or 0.03 (**B** and **C**) with washed cells from M9

437 overnight cultures grown with succinate in the absence (**A**) or presence (**B** and **C**) of

438 kanamycin and 0.2% rhamnose as inducer for the plasmids pJEM[PedR2] and

439 pJEM[PedR2^{D53A}]. **A**) Growth of Δ*pedE* (black circles), Δ*pedE*_PedS2^{S178P} (orange dots), and

440 Δ*pedE*_PedS2^{S178P}Δ*pedR2* (grey dots). **B**) Growth of Δ*pedH*_PedS2^{S178P}Δ*pedR2* harboring

441 pJEM[PedR2] (grey dots) or pJEM[PedR2^{D53A}] (orange dots). **C**) Growth of

442 Δ*pedE*_PedS2^{S178P}Δ*pedR2* harboring pJEM[PedR2] (grey dots) or pJEM[PedR2^{D53A}] (orange

443 dots). Data points represent the mean of biological triplets and error bars correspond to the

444 respective standard deviations (positive error values).

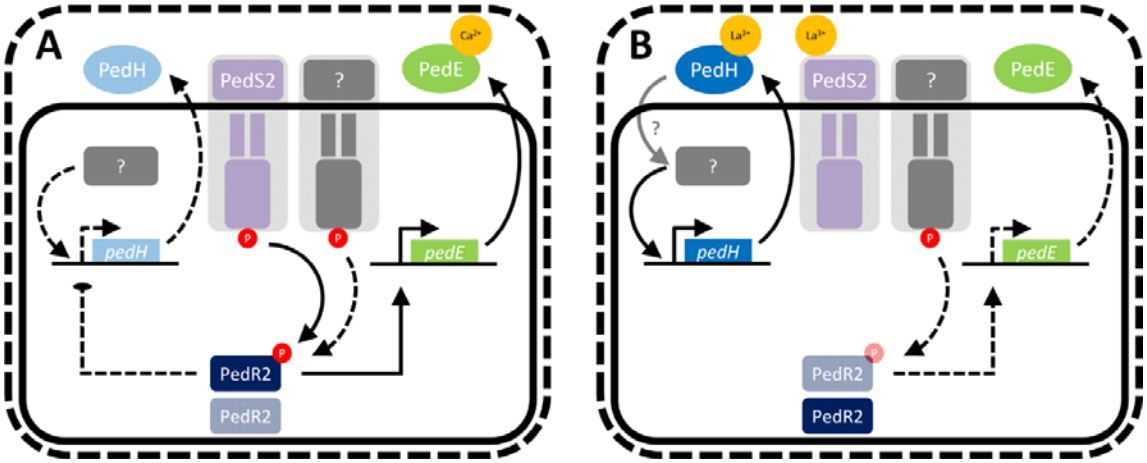

Figure 5: Working hypothesis of REE-mediated switch of *pedE* and *pedH* in *Pseudomonas putida* KT2440. Black lines indicate known regulations or functionalities. Grey boxes with question marks indicate unknown regulatory components. Solid lines indicate a strong regulatory effect on genes or production of enzymes, whereas dotted lines indicate weaker regulatory effects or low production of enzymes. A detailed description of the working model is given in the text.

452 ## References

453 Agrawal, R., Sahoo, B.K., and Saini, D.K. (2016) Cross-talk and specificity in two-component
454 signal transduction pathways. *Future Microbiol.* **11**: 685–697.

455 Anthony, C. (2001) Pyrroloquinoline Quinone (PQQ) and Quinoprotein Enzymes. *Antioxid.*
456 *Redox Signal.* **3**: 757–774.

457 Arias, S., Olivera, E.R., Arcos, M., Naharro, G., and Luengo, J.M. (2008) Genetic analyses and
458 molecular characterization of the pathways involved in the conversion of 2-
459 phenylethylamine and 2-phenylethanol into phenylacetic acid in *Pseudomonas putida*
460 U. *Environ. Microbiol.* **10**: 413–432.

461 Bourret, R.B., Hess, J.F., and Simon, M.I. (1990) Conserved aspartate residues and
462 phosphorylation in signal transduction by the chemotaxis protein CheY. *Proc. Natl.*
463 *Acad. Sci.* **87**: 41–45.

464 Choi, K.-H., Gaynor, J.B., White, K.G., Lopez, C., Bosio, C.M., Karkhoff-Schweizer, R.R., and
465 Schweizer, H.P. (2005) A Tn7-based broad-range bacterial cloning and expression
466 system. *Nat. Methods* **2**: 443–448.

467 Chu, F., Beck, D.A.C., and Lidstrom, M.E. (2016) MxaY regulates the lanthanide-mediated
468 methanol dehydrogenase switch in *Methylomicrobium buryatense*. *PeerJ* **4**: e2435.

469 Chu, F. and Lidstrom, M.E. (2016) XoxF Acts as the Predominant Methanol Dehydrogenase in
470 the Type I Methanotroph *Methylomicrobium buryatense*. *J. Bacteriol.* **198**: 1317–1325.

471 van Dam, N.M., Weinhold, A., and Garbeva, P. (2016) Calling in the Dark: The Role of
472 Volatiles for Communication in the Rhizosphere. In, Blande,J.D. and Glinwood,R. (eds),
473 *Deciphering Chemical Language of Plant Communication*. Springer International
474 Publishing, Cham, pp. 175–210.

475 Farhan Ul Haque, M., Kalidass, B., Bandow, N., Turpin, E.A., DiSpirito, A.A., and Semrau, J.D.

476 (2015) Cerium Regulates Expression of Alternative Methanol Dehydrogenases in
477 *Methylosinus trichosporium* OB3b. *Appl. Environ. Microbiol.* **81**: 7546–7552.
478 Fitriyanto, N.A., Fushimi, M., Matsunaga, M., Pertiwiningrum, A., Iwama, T., and Kawai, K.
479 (2011a) Molecular structure and gene analysis of Ce3+ -induced methanol
480 dehydrogenase of *Bradyrhizobium* sp. MAFF211645. *J. Biosci. Bioeng.* **111**: 613–7.
481 Fitriyanto, N.A., Nakamura, M., Muto, S., Kato, K., Yabe, T., Iwama, T., et al. (2011b) Ce3+-
482 induced exopolysaccharide production by *Bradyrhizobium* sp. MAFF211645. *J. Biosci.*
483 *Bioeng.* **111**: 146–152.
484 Gibson, D.G. (2011) Enzymatic Assembly of Overlapping DNA Fragments. In, *Methods in*
485 *Enzymology*., pp. 349–361.
486 Good, N.M., Vu, H.N., Suriano, C.J., Subuyuj, G.A., Skovran, E., and Martinez-Gomez, N.C.
487 (2016) Pyrroloquinoline Quinone Ethanol Dehydrogenase in *Methylobacterium*
488 *extorquens* AM1 Extends Lanthanide-Dependent Metabolism to Multicarbon
489 Substrates. *J. Bacteriol.* **198**: 3109–3118.
490 Good, N.M., Walser, O.N., Moore, R.S., Suriano, C., Huff, A.F., and Martinez-Gomez, N.C.
491 (2018) Investigation of lanthanide-dependent methylotrophy uncovers complementary
492 roles for alcohol dehydrogenase enzymes. *bioRxiv*.
493 Graf, N. and Altenbuchner, J. (2011) Development of a method for markerless gene deletion
494 in *Pseudomonas putida*. *Appl. Environ. Microbiol.* **77**: 5549–5552.
495 Gu, W. and Semrau, J.D. (2017) Copper and cerium-regulated gene expression in
496 *Methylosinus trichosporium* OB3b. *Appl. Microbiol. Biotechnol.* **101**: 8499–8516.
497 Insam, H. and Seewald, M.S.A. (2010) Volatile organic compounds (VOCs) in soils. *Biol. Fertil.*
498 *Soils* **46**: 199–213.
499 Jeske, M. and Altenbuchner, J. (2010) The *Escherichia coli* rhamnose promoter rhaP BAD is in

500 *Pseudomonas putida* KT2440 independent of Crp–cAMP activation. *Appl. Microbiol.*
501 *Biotechnol.* **85**: 1923–1933.
502 Van Kessel, J.C., Rutherford, S.T., Shao, Y., Utria, A.F., and Bassler, B.L. (2013) Individual and
503 combined roles of the master regulators apha and luxr in control of the *Vibrio harveyi*
504 quorum-sensing regulon. *J. Bacteriol.* **195**: 436–443.
505 Letunic, I. and Bork, P. (2018) 20 years of the SMART protein domain annotation resource.
506 *Nucleic Acids Res.* **46**: D493–D496.
507 Lv, H., Sahin, N., and Tani, A. (2018) Isolation and genomic characterization of
508 *Novimethylophilus kurashikiensis* gen. nov. sp. nov., a new lanthanide-dependent
509 methylotrophic species of *Methylophilaceae*. *Environ. Microbiol.* **20**: 1204–1223.
510 Maniatis, T., Fritsch, E., Sambrook, J., and Laboratory, C.S.H. (1982) Molecular Cloning: A
511 Laboratory Manual Cold Spring Harbor, N.Y. Cold Spring Harbor Laboratory.
512 Masuda, S., Suzuki, Y., Fujitani, Y., Mitsui, R., Nakagawa, T., Shintani, M., and Tani, A. (2018)
513 Lanthanide-Dependent Regulation of Methylotrophy in *Methylobacterium aquaticum*
514 Strain 22A. *mSphere* **3**: e00462-17.
515 Mern, D.S., Ha, S.W., Khodaverdi, V., Gliese, N., and Gorisch, H. (2010) A complex regulatory
516 network controls aerobic ethanol oxidation in *Pseudomonas aeruginosa*: indication of
517 four levels of sensor kinases and response regulators. *Microbiology* **156**: 1505–1516.
518 Milani, M., Leoni, L., Rampioni, G., Zennaro, E., Ascenzi, P., and Bolognesi, M. (2005) An
519 active-like structure in the unphosphorylated StyR response regulator suggests a
520 phosphorylation-dependent allosteric activation mechanism. *Structure* **13**: 1289–1297.
521 Mückschel, B., Simon, O., Klebensberger, J., Graf, N., Rosche, B., Altenbuchner, J., et al.
522 (2012) Ethylene glycol metabolism by *Pseudomonas putida*. *Appl. Environ. Microbiol.*
523 **78**: 8531–9.

524 Nakagawa, T., Mitsui, R., Tani, A., Sasa, K., Tashiro, S., Iwama, T., et al. (2012) A Catalytic Role
525 of XoxF1 as La3+-Dependent Methanol Dehydrogenase in *Methylobacterium*
526 *extorquens* Strain AM1. *PLoS One* **7**: e50480.
527 Parkinson, J.S. (2010) Signaling Mechanisms of HAMP Domains in Chemoreceptors and
528 Sensor Kinases. *Annu. Rev. Microbiol.* **64**: 101–122.
529 Penuelas, J., Asensio, D., Tholl, D., Wenke, K., Rosenkranz, M., Piechulla, B., and Schnitzler,
530 J.P. (2014) Biogenic volatile emissions from the soil. *Plant. Cell Environ.* **37**: 1866–1891.
531 Pol, A., Barends, T.R.M., Dietl, A., Khadem, A.F., Eygensteyn, J., Jetten, M.S.M., and Op den
532 Camp, H.J.M. (2014) Rare earth metals are essential for methanotrophic life in volcanic
533 mudpots. *Environ. Microbiol.* **16**: 255–264.
534 Regenhardt, D., Heuer, H., Heim, S., Fernandez, D.U., Strompl, C., Moore, E.R.B., and Timmis,
535 K.N. (2002) Pedigree and taxonomic credentials of *Pseudomonas putid*a strain KT2440.
536 *Environ. Microbiol.* **4**: 912–915.
537 Rowland, M.A. and Deeds, E.J. (2014) Crosstalk and the evolution of specificity in two-
538 component signaling. *Proc. Natl. Acad. Sci.* **111**: 5550–5555.
539 Sarkar, B. (2002) Heavy Metals in the Environment CRC Press.
540 Schobert, M. and Görisch, H. (2001) A soluble two-component regulatory system controls
541 expression of quinoprotein ethanol dehydrogenase (QEDH) but not expression of
542 cytochrome c(550) of the ethanol-oxidation system in *Pseudomonas aeruginosa*.
543 *Microbiology* **147**: 363–372.
544 Semrau, J.D., DiSpirito, A.A., Gu, W., and Yoon, S. (2018) Metals and Methanotrophy. *Appl.*
545 *Environ. Microbiol.* **84**: e02289-17.
546 Shiller, A.M., Chan, E.W., Joung, D.J., Redmond, M.C., and Kessler, J.D. (2017) Light rare earth
547 element depletion during Deepwater Horizon blowout methanotrophy. *Sci. Rep.* **7**:

548 10389.

549 Sievers, F., Wilm, A., Dineen, D., Gibson, T.J., Karplus, K., Li, W., et al. (2014) Fast, scalable
550 generation of high-quality protein multiple sequence alignments using Clustal Omega.
551 *Mol. Syst. Biol.* **7**: 539–539.

552 Singh, V.S., Dubey, A.P., Gupta, A., Singh, S., Singh, B.N., and Tripathi, A.K. (2017) Regulation
553 of a Glycerol-Induced Quinoprotein Alcohol Dehydrogenase by σ 54 and a LuxR-Type
554 Regulator in *Azospirillum brasilense* Sp7. *J. Bacteriol.* **199**: e00035-17.

555 Skovran, E., Palmer, A.D., Rountree, A.M., Good, N.M., and Lidstrom, M.E. (2011) XoxF Is
556 Required for Expression of Methanol Dehydrogenase in *Methylobacterium extorquens*
557 AM1. *J. Bacteriol.* **193**: 6032–6038.

558 Springer, A.L., Auman, A.J., and Lidstrom, M.E. (1998) Sequence and characterization of
559 mxaB, a response regulator involved in regulation of methanol oxidation, and of mxaW,
560 a methanol-regulated gene in *Methylobacterium extorquens* AM1. *FEMS Microbiol. Lett.*
561 **160**: 119–24.

562 Springer, A.L., Morris, C.J., and Lidstrom, M.E. (1997) Molecular analysis of mxbD and mxbM,
563 a putative sensor-regulator pair required for oxidation of methanol in
564 *Methylobacterium extorquens* AM1. *Microbiology* **143**: 1737–1744.

565 Stock, A.M., Robinson, V.L., and Goudreau, P.N. (2000) Two-Component Signal Transduction.
566 *Annu. Rev. Biochem.* **69**: 183–215.

567 Taubert, M., Grob, C., Howat, A.M., Burns, O.J., Dixon, J.L., Chen, Y., and Murrell, J.C. (2015)
568 XoxF encoding an alternative methanol dehydrogenase is widespread in coastal marine
569 environments. *Environ. Microbiol.* **17**: 3937–3948.

570 Toyama, H., Mathews, F.S., Adachi, O., and Matsushita, K. (2004) Quinohemoprotein alcohol
571 dehydrogenases: structure, function, and physiology. *Arch. Biochem. Biophys.* **428**: 10–

572 21.

573 Vekeman, B., Speth, D., Wille, J., Cremers, G., De Vos, P., Op den Camp, H.J.M., and Heylen,
574 K. (2016) Genome Characteristics of Two Novel Type I Methanotrophs Enriched from
575 North Sea Sediments Containing Exclusively a Lanthanide-Dependent XoxF5-Type
576 Methanol Dehydrogenase. *Microb. Ecol.* **72**: 503–509.

577 Vu, H.N., Subuyuj, G.A., Vijayakumar, S., Good, N.M., Martinez-Gomez, N.C., and Skovran, E.
578 (2016) Lanthanide-Dependent Regulation of Methanol Oxidation Systems in
579 *Methylobacterium extorquens* AM1 and Their Contribution to Methanol Growth. *J.*
580 *Bacteriol.* **198**: 1250–1259.

581 Wackett, L.P. (2003) Pseudomonas putida- a versatile biocatalyst. *Nat. Biotechnol.*

582 Waters, C.M. and Bassler, B.L. (2006) The *Vibrio harveyi* quorum-sensing system uses shared
583 regulatory components to discriminate between multiple autoinducers. *Genes Dev.* **20**:
584 2754–2767.

585 Wehrmann, M., Billard, P., Martin-Meriadec, A., Zegeye, A., and Klebensberger, J. (2017)
586 Functional Role of Lanthanides in Enzymatic Activity and Transcriptional Regulation of
587 Pyrroloquinoline Quinone-Dependent Alcohol Dehydrogenases in *Pseudomonas putida*
588 KT2440. *MBio* **8**: e00570-17.

589 Winsor, G.L., Griffiths, E.J., Lo, R., Dhillon, B.K., Shay, J.A., and Brinkman, F.S.L. (2016)
590 Enhanced annotations and features for comparing thousands of *Pseudomonas* genomes
591 in the *Pseudomonas* genome database. *Nucleic Acids Res.* **44**: D646–D653.

592 Wu, X., Monchy, S., Taghavi, S., Zhu, W., Ramos, J., and van der Lelie, D. (2011) Comparative
593 genomics and functional analysis of niche-specific adaptation in *Pseudomonas putida*.
594 *FEMS Microbiol. Rev.* **35**: 299–323.

595 Xu, H.H., Janka, J.J., Viebahn, M., and Hanson, R.S. (1995) Nucleotide sequence of the mxcQ

596 and mxcE genes, required for methanol dehydrogenase synthesis in *Methylobacterium*
597 *organophilum* XX: a two-component regulatory system. *Microbiology* **141**: 2543–2551.
598 Zheng, Y., Huang, J., Zhao, F., and Chistoserdova, L. (2018) Physiological Effect of XoxG(4) on
599 Lanthanide-Dependent Methanotrophy. *MBio* **9**: e02430-17.
600